AIAA Journal
Vol. 49, No. 11, November 2011

Technical Notes

Control-Oriented Design Using Surrogate-Based Optimization and Existence Conditions for Robust Performance

Sanketh Bhat* and Rick Lind†
University of Florida, Gainesville, Florida 32611

DOI: 10.2514/1.J050700

I. Introduction

MISSION capability of a vehicle is ultimately evaluated by closed-loop performance. Such capability depends on a synergistic integration of aerodynamics, structures, propulsion, and control, which results in flight dynamics that are optimal for the mission. Unfortunately, most systems such as aircraft are traditionally designed using a sequential series of open-loop optimizations that cannot account for, or optimize, any synergistic integrations. A formulation for design that inherently considers control must therefore be developed to enable optimal closed-loop performance.

The issue of cost function is actually quite critical to the inclusion of control synthesis for design optimization. Every discipline has metrics that are unique to their objectives, so a single cost that encompasses all these metrics can be challenging to formulate. One approach that considers vibration control uses norms, both for vibration level and effort, as a cost in a linear-quadratic framework [1]. A mixed-norm approach is formulated that considers both $\mathcal{H}_2$ and $\mathcal{H}_\infty$ in summation to represent independent metrics of the design [2]. A positive-real condition across frequency is also introduced as a cost that has time-domain interpretations for design [3].

Several formulations formulate cost functions and solution methodologies for designs that include linear matrix inequalities (LMIs) associated with $\mathcal{H}_\infty$-norm synthesis. One generates a nonconvex formulation and uses iterations to solve the associated optimization [4]. Another approximates functions associated with perturbed state-space matrices as LMIs to be solved using an iterative approach [5]. A two-step procedure is used for an optimization coupled with an LMI solver for the controller [6] as an multidisciplinary optimization approach. Another approach considers an iterative sequential control design and a coupled redesign with each iteration involving the solution of an LMI [7].

This Note introduces a control-oriented approach for design that avoids the common difficulties of simultaneous structure-control design, which is known to be nonconvex [8–11]. The approach actually considers an existence question that notes if a controller exists for a given structure that achieves a desired level of performance. The approach does not design both the structure and control to optimize a closed-loop norm; rather, it designs a structure for which a controller exists that optimizes a closed-loop norm. Formulations using control synthesis to minimize an $\mathcal{H}_\infty$-norm metric and an $\mathcal{H}_2$-norm are derived using their appropriate existence conditions. As important, a solution methodology is used based on surrogate modeling to avoid the iterations and expensive computations associated with techniques doing design with LMI expressions. The surrogate-based optimization is shown to be efficient and effective and exploring a design space to optimize the closed-loop metric.

II. Closed-Loop Design Space

Systems are evaluated on their ability to perform missions; consequently, the design space must include all variables that affect such ability. The closed-loop operation of such systems suggests a decomposition of the design space into separate subspaces relating the plant dynamics and the controller.

A space of design parameters $\mathbb{P}$ relates the variables such as geometry, structure, materials, and other aspects that affect the open-loop dynamics. The associated plant models are formulated as state-space systems with a matrix quadruple of

$$\left\{A, [B_1 B_2], \begin{bmatrix} C_1 \\ C_2 \end{bmatrix}, \begin{bmatrix} 0 & D_{12} \\ D_{21} & 0 \end{bmatrix}\right\}$$

Each of these elements is allowed to be a function of the design parameters.

The controller in this formulation is restricted to minimizing either the $\mathcal{H}_\infty$ norm or the $\mathcal{H}_2$ norm of the closed-loop system. The associated controllers are determined by the matrices of the state-space systems along with a pair of matrices that solve Riccati equations. As such, the design space relating the controller is simply positive-definite matrices.

III. Feasibility-Based Optimization

A. $\mathcal{H}_\infty$ Control Synthesis

The metric for design can be cast as an $\mathcal{H}_\infty$-norm condition on the transfer function from disturbances to errors for a closed-loop system. As such, the design seeks to find the optimal values for both the open-loop dynamics and a controller to minimize the $\mathcal{H}_\infty$-norm of γ, as formulated in Eq. (1):

$$\begin{aligned}
&\min_{\pi\in\mathbb{P}} \gamma \\
&X = X^* > 0 \\
&Y = Y^* > 0 \\
&\text{subject to} \\
&0 = XA(\pi) + A(\pi)^*X + X\left(\frac{1}{\gamma^2}B_1(\pi)B_1(\pi)^* - B_2(\pi)B_2(\pi)^*\right)X + C_1(\pi)^*C_1(\pi) \\
&0 = A(\pi)Y + YA(\pi)^* + Y\left(\frac{1}{\gamma^2}C_1(\pi)^*C_1(\pi) - C_2(\pi)^*C_2(\pi)\right)Y + B_1(\pi)B_1(\pi)^* \\
&\gamma^2 > \rho(XY)
\end{aligned} \tag{1}$$

B. $\mathcal{H}_2$ Control Synthesis

A metric can also be expressed as the $\mathcal{H}_2$-norm condition on the closed-loop system. Such a gain again reflects the performance as

Received 15 June 2010; revision received 16 June 2011; accepted for publication 27 June 2011.

*Research Assistant, Department of Mechanical and Aerospace Engineering; sanketh@ufl.edu. Student Member AIAA.

†Associate Professor, Department of Mechanical and Aerospace Engineering; ricklind@ufl.edu. Associate Fellow AIAA.

size of errors given disturbances, so a decrease in norm indicates an increase in performance. The resulting optimization is formulated in Eq. (2) as minimizing the norm γ while searching over the open-loop variables π and the solutions X and Y associated with the existence conditions for a controller. Note that a pair of variables is introduced as $R_1 = D_{12}^* D_{12}$ and $R_2 = D_{21} D_{21}$:

$$\min_{\pi \in \mathbb{P}} \gamma$$

$$X = X^* > 0$$

$$Y = Y^* > 0$$

subject to

$$\begin{aligned} 0 &= X(A(\pi) - B_2(\pi)R_1(\pi)^{-1}D_{12}(\pi)C_1(\pi)) + (A(\pi) \\ &\quad - B_2(\pi)R_1(\pi)^{-1}D_{12}(\pi)^*C_1(\pi))^*X \\ &\quad - XB_2(\pi)R_1(\pi)^{-1}B_2(\pi)X + C_1(\pi)^*(I - D_{12}R_1^{-1}D_{12}^*C_1^*)C_1(\pi) \\ 0 &= Y(A(\pi) - B_1(\pi)D_{21}(\pi)^*R_2(\pi)^{-1}C_2(\pi))^* + (A(\pi) \\ &\quad - B_1(\pi)D_{21}(\pi)^*R_2(\pi)^{-1}C_2(\pi))Y - YC_2(\pi)R_2(\pi)^{-1}C_2(\pi)Y \\ &\quad + B_1(\pi)(I - D_{21}^*R_2^{-1}D_{21})B_1(\pi)^* \end{aligned} \tag{2}$$

IV. Surrogate-Based Design Optimization

Surrogate models, also known as metamodels, are developed as approximations of parametrized models across a design space. These models provide information that is suitable for design optimization, but they incur a computational expense that is dramatically less than would be required to evaluate the high-fidelity model [12–14]. Several methods for generating these surrogate models are developed including kriging, support vector regression (SVR), radial basis neutral network (RBNN), and polynomial response surface .[‡]

The approach of kriging has particular interest for surrogate modeling. All approaches have value with respect to accuracy; however, only a limited few such as kriging provide statistics associated with anticipated accuracy. In this case, kriging provides the prediction of the cost, $\hat{\gamma}(\pi)$ and the associated prediction variance, $\sigma^2(\pi)$, at every point in the design space. A difference parameter is computed that relates the cost of the current best configuration, γ_{best}, and the predicted cost at every point in the design space, which is given as u in Eq. (3):

$$u(\pi) = (\gamma_{\text{best}} - \hat{\gamma}(\pi))/\sigma(\pi) \tag{3}$$

An algorithm known as efficient global optimization (EGO) is developed to use the statistics associated with kriging for exploring a design space using multiple types of surrogate models [15–18]. The fundamental concept is to increase the initial number of expensive-to-compute configurations by adding a select few at ideal locations that will improve the overall accuracy of the easy-to-compute surrogate model. These locations are found using a function of expected improvement, $E(I(\pi))$, that estimates how much the surrogate could be improved by adding a design at the configuration of π. Such a function is given in Eq. (4) using the Φ as the cumulative density function and ϕ as the probability density function for a normal distribution:

$$E[I(\pi)] = \sigma(\pi)(u\Phi(u) + \phi(\pi)) \tag{4}$$

V. Example

A. Objective

A control-oriented design is optimized for a hypersonic vehicle to minimize aerothermoelastic effects. Such effects are initially caused by coupling between the propulsion dynamics of the engine and the structural dynamics of the fuselage. The challenge is compounded by the introduction of thermal gradients that result from the tremendous heating across the fuselage throughout flight. As such, vibration attenuation becomes a critical aspect of mission performance.

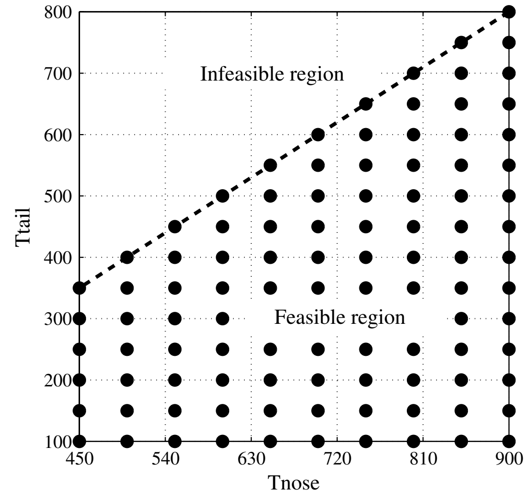

Fig. 1 Thermal profiles comprising the design space.

A baseline vehicle is adopted from an extensive program by the U.S. Air Force for a reduced-order model [19–26]. This model includes five states for the rigid-body flight dynamics and an additional six states associated with three flexible-body structural dynamics. The model is particularly attractive in that it contains a rigorous derivation of the aerothermoelastic coupling that explicitly highlights the effects of vibrations on mission performance [27].

B. Design Space

The design space for the open-loop dynamics consists of a two-dimensional set $\mathbb{P}$ related to effective temperatures $[T_{\text{nose}}, T_{\text{tail}}]$ of the fuselage structure at the nose and tail. The design is actually choosing the amount of thermal protection system on the structure; however, the effective temperatures are a direct result of that thermal protection system and thus represent the design parameters. The set of effective temperatures in the design space are limited to configurations with monotonic decrease from the nose to the tail, as shown in Fig. 1.

The temperatures are noted as effective because the surface temperatures of the vehicle will be exceedingly high, but the temperature of the fuselage structure will be noticeably cooler [28,29]. In this case, a reduced-order model of the fuselage is generated as a titanium beam, so the range of effective temperatures used in Fig. 1 is thus limited by material properties of titanium. The effective temperatures in the design space are actually introduced to the structural dynamics through variations in Young's modulus.

The open-loop dynamics are parametrized as function of these effective temperatures. Elements of the linearized state-space models

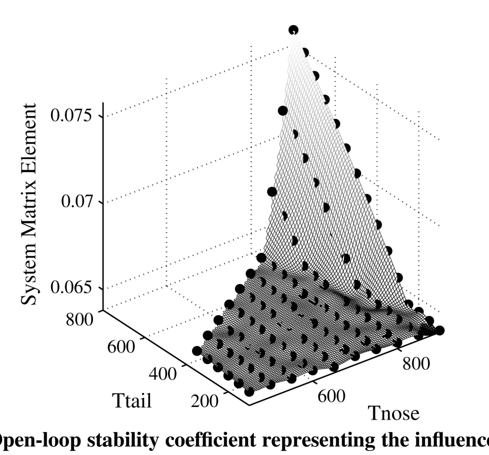

Fig. 2 Open-loop stability coefficient representing the influence of the velocity on the velocity of the first bending mode as a function of design space.

[‡]Data available online at http://sites.google.com/site/felipeacviana/ [retrieved 5 September 2011].

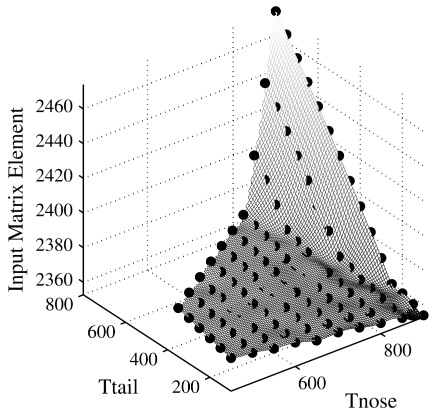

Fig. 3 Open-loop control coefficient representing the influence of the elevator deflection on the velocity of the first bending mode as a function of design space.

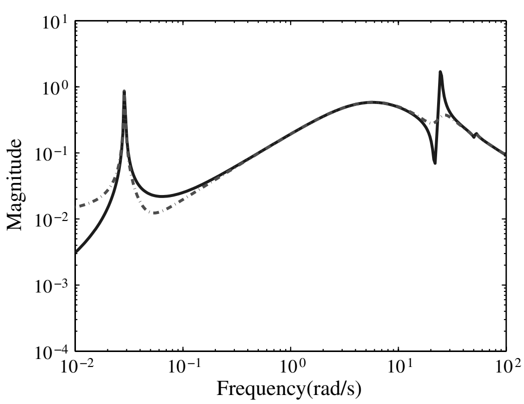

Fig. 4 Transfer function from elevator deflection to pitch rate for the nominal (solid line) and target model (dash-dotted line).

indicate the nonlinear dependency on the design space. A set of variables that are representative of this dependency is noted in Fig. 2 for the influence of airspeed on the bending-mode velocity used in the state matrix and in Fig. 3 for the influence of elevator on the bending-mode velocity used in the control-effectiveness matrix. Such dependencies arise with the data in Fig. 2 as the row-7 and column-1 element of the state matrix that indicates how the first state, airspeed, affects the derivative of the seventh state, bending-mode velocity. Similarly, the data in Fig. 3 are the row-7 and column-1 element of the input matrix that indicates how the first input, elevator, affects the derivative of the seventh state. These values indicate that the aeroservoelastic coupling shown in Fig. 2 is large, as is the control effectiveness shown in Fig. 3 for configurations with high temperatures at both nose and tail. Such dependency makes design challenging, since an ideal configuration should have small coupling but large effectiveness.

C. Performance Objective

A model-matching approach is chosen to specify a desired level of vibration attenuation. As such, a target model represents dynamics with appropriate damping on the structural mode. The transfer functions are shown in Fig. 4 for the nominal open-loop dynamics and the target dynamics. Note that the peak near 0.04 rad/s is associated with a rigid-body flight mode, whereas the peak near 22 rad/s is associated with the structural mode that should be attenuated.

D. Control-Oriented Design

1. Global Search

The technique of global search is used to find the optimal design. In this case, a controller is computed for each of the potential profiles in Fig. 1. Thus, a total of 105 controllers were computed to generate the associated closed-loop norm associated with vibration attenuation, as shown in Fig. 5 for $\mathcal{H}_\infty$-norm performance and $\mathcal{H}_2$-norm performance.

The variations across the design space in Fig. 5 show some interesting differences between the two norms. Certainly, both have a general nonlinear relationship that peaks at a configuration associated with the hottest temperatures for nose and tail; however, other important trends are dissimilar. The magnitude of variation is quite disparate in that the use $\mathcal{H}_\infty$ as the norm shows only a 2.2% variation across the design space, whereas the use of $\mathcal{H}_2$ as the norm shows a large 29.1% variation. Also, the closed-loop norms associated with the largest thermal gradients are roughly decreasing in terms of $\mathcal{H}_\infty$ as the gradient gets larger, but vary sporadically in terms of $\mathcal{H}_2$.

The resulting configurations that are optimal are $\pi = [900, 100]$ with respect to the closed-loop $\mathcal{H}_\infty$ norm and $\pi = [600, 100]$ with respect to the closed-loop $\mathcal{H}_2$ norm. The associated norms are 0.22 as measured by $\mathcal{H}_\infty$ and 0.69 as measured by $\mathcal{H}_2$. The values of these norms being less than one guarantees that the performance objectives are achieved for these designs.

2. Surrogate-Based Design Optimization

The use of surrogate models is evaluated to optimize the design with low computational cost. In this case, a random set of 15 configurations is chosen from the 105 possibilities in Fig. 1. Surrogate models are computed using kriging along with RBNN and SVR with various types of radial basis functions (RBFs), as given in Table 1.

The EGO approach uses minimal computations to optimize the designs to be the same configurations as are found by the computationally expensive global search (see footnote ‡). The implementation always chooses a surrogate from kriging along with the surrogate from Table 1 that generates the lowest estimate of

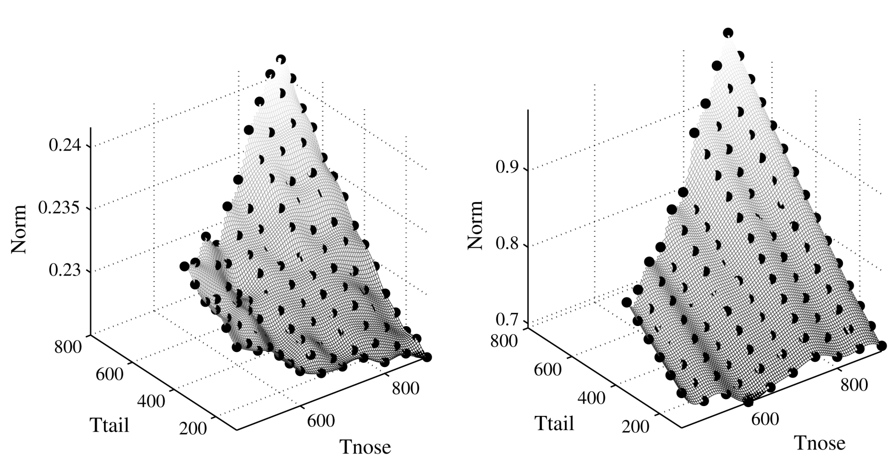

Fig. 5 Closed-loop norm for $\mathcal{H}_\infty$ (left) and $\mathcal{H}_2$ (right) across the design space.

Table 1 Types of surrogate models

Number	Candidate surrogate
1	RBNN
2	SVR exponential RBF
3	SVR linear RBF
4	SVR polynomial RBF
5	SVR Gaussian RBF
6	SVR linear spline RBF
7	SVR analysis of variance B-spline RBF

Table 2 Surrogate-based design optimization using multiple surrogates for $\mathcal{H}_\infty$ synthesis

Case	Surrogate 1	Surrogate 2	Initial best solution $[T_{\mathrm{nose}}, T_{\mathrm{tail}}]$	Final best solution $[T_{\mathrm{nose}}, T_{\mathrm{tail}}]$
A	Kriging	SVR Gaussian RBF	[850, 150]	[900, 100]
B	Kriging	SVR polynomial	[850, 150]	[900, 100]
C	Kriging	SVR polynomial	[750, 150]	[900, 100]

Table 3 Surrogate-based design optimization using multiple surrogates for $\mathcal{H}_2$ synthesis

Case	Surrogate 1	Surrogate 2	Initial best solution $[T_{\mathrm{nose}}, T_{\mathrm{tail}}]$	Final best solution $[T_{\mathrm{nose}}, T_{\mathrm{tail}}]$
D	Kriging	SVR polynomial	[900, 100]	[600, 100]
E	Kriging	SVR linear spline	[800, 150]	[600, 100]
F	Kriging	SVR linear spline	[900, 100]	[600, 100]

cross-validations errors, which estimates accuracy of the surrogate, known as the PRESSRMS value [15]. The design is initiated with three different sets of 15 randomly chosen configurations whose optimal closed-loop norm is given in Table 2 for $\mathcal{H}_\infty$ and in Table 3 for $\mathcal{H}_2$. The tables also list the second surrogate that had the lowest PRESSRMS value and the final configuration of the optimal design.

VI. Conclusions

Simultaneous design of an open-loop plant and controller is exceedingly challenging. A control-oriented design is introduced that does not actually compute both the plant and controller; rather, the plant is determined for which a controller exists that minimizes a closed-loop norm. The concept uses existence conditions for the controller that can be parametrized around a design space. The actual optimization results from efficient exploration of that design space using surrogate modeling. A representative model of a hypersonic vehicle is used to demonstrate this approach can indeed generate an optimal design.

Acknowledgment

This work was supported through NASA NNX07AC46A with Donald Soloway as Program Manager.

References

[1] Messac, A., and Malek, K., "Control-Structure Integrated Design," *AIAA Journal*, Vol. 30, No. 8, 1992, pp. 2124–2131. doi:10.2514/3.11190

[2] Lu, J., and Skelton, R. E., "Integrating Structure and Control Design to Achieve Mixed $\mathcal{H}_2/\mathcal{H}_\infty$ Performance," *International Journal of Control*, Vol. 73, 2000, pp. 1449–1462. doi:10.1080/00207170050163323

[3] Iwasaki, T., Hara, S., and Yamauchi, H., "Structure/Control Design Integration with Finite Frequency Positive Real Property," *Proceedings of the American Control Conference*, IEEE Press, Piscataway, NJ, 2000, pp. 549–533.

[4] Niewoehner, R. J., and Kaminer, I. I., "Integrated Aircraft-Controller Design Using Linear Matrix Inequalities," *Journal of Guidance, Control, and Dynamics*, Vol. 19, No. 2, 1996, pp. 445–452. doi:10.2514/3.21638

[5] Hiramoto, K., and Grigoriadis, K. M., "Integrated Design of Structural and Control Systems with a Homotopy-Like Iterative Method," *International Journal of Control*, Vol. 79, No. 9, 2006, pp. 1062–1073. doi:10.1080/00207170600750105

[6] Kajiwara, I., and Haftka, R. T., "Integrated Design of Aerodynamics and Control System for Micro Aerial Vehicles," *JSME International Journal, Series C*, Vol. 43, No. 3, 2000, pp. 684–690.

[7] Grigoriadis, K. M., and Skelton, R. E., "Integrated Structural and Control Design for Vector Second-Order Systems via LMIs," *Proceedings of the 1998 American Control Conference*, IEEE Press, Piscataway, NJ, 1998, pp. 1625–1629.

[8] Safonov, M. G., Goh, K. C., and Ly, J. H., "Control System Synthesis via Bilinear Matrix Inequalities," *IEEE American Control Conference*, IEEE Press, Piscataway, NJ, 1994, pp. 45–49.

[9] Shi, G., and Skelton, R. E., "An Algorithm for Integrated Structure and Control Design with Variance Bounds," *IEEE Conference on Decision and Control*, IEEE Press, Piscataway, NJ, 1996, pp. 167–172.

[10] Tanaka, T., and Sugie, T., "General Framework and BMI Formulae for Simultaneous Design of Structure and Control Systems," *IEEE Conference on Decision and Control*, IEEE Press, Piscataway, NJ, 1997, pp. 773–778.

[11] Tuan, H. D., and Apkarian, P., "Low Nonconvexity-Rank Bilinear Matrix Inequalities: Algorithms and Applications in Robust Controller and Structure Design," *IEEE Transactions on Automatic Control*, Vol. 45, No. 11, Nov. 2000, pp. 2111–2117. doi:10.1109/9.887636

[12] Sacks, J., Welch, W. J., Mitchell, T. J., and Wynn, H. P., "Design and Analysis of Computer Experiments," *Statistical Science*, Vol. 4, No. 4, 1989, pp. 409–435. doi:10.1214/ss/1177012413

[13] Queipo, N. V., Haftka, R. T., Shyy, W., Goel, T., Vaidyanathan, R., and Tucker, P. K., "Surrogate-Based Analysis and Optimization," *Progress in Aerospace Sciences*, Vol. 41, 2005, pp. 1–28. doi:10.1016/j.paerosci.2005.02.001

[14] Simpson, T. W., Toropov, V., Balabanov, V., and Viana, F. A. C., "Design and Analysis of Computer Experiments in Multidisciplinary Design Optimization: A Review of How Far We Have Come—or Not," AIAA/ISSMO Multidisciplinary Analysis and Optimization Conference, AIAA Paper 2008-5802, 2008.

[15] Jones, D., Schonlau, M., and Welch, W., "Efficient Global Optimization of Expensive Black-Box Functions," *Journal of Global Optimization*, Vol. 13, No. 4, 1998, pp. 455–492. doi:10.1023/A:1008306431147

[16] Stein, M. L., *Interpolation of Spatial Data: Some Theory for Kriging*, Springer, New York, 1999.

[17] Martin, J. D., and Simpson, T. W., "Use of Kriging Models to Approximate Deterministic Computer Models," *AIAA Journal*, Vol. 43, No. 4, 2005, pp. 853–863. doi:10.2514/1.8650

[18] Kleijnen, J. P. C.,"Kriging Metamodeling in Simulation: A Review," *European Journal of Operational Research*, Vol. 192, No. 3, 2009, pp. 707–716.

[19] Bolender, M., and Doman, D., "A nonlinear Model for the Longitudinal Dynamics of a Hypersonic Air-Breathing Vehicle," AIAA Guidance, Navigation, and Control Conference, AIAA Paper 2005-6255, 2005.

[20] Bolender, M., and Doman, D., "Nonlinear Longitudinal Dynamical Model of an Air-Breathing Hypersonic Vehicle," *Journal of Spacecraft and Rockets*, Vol. 44, No. 2, March–April 2007, pp. 374–387. doi:10.2514/1.23370

[21] Bolender, M., and Doman, D., "Modeling Unsteady Heating Effects on the Strucutral Dynamics of a Hypersonic Vehicle," AIAA Atmospheric Flight Mechanics Conference, AIAA Paper 2006-6646, 2006.

[22] Williams, T., Bolender, M., Doman, D., and Morataya, O., "An Aerothermal Flexible Model Analysis of a Hypersonic Vehicle," AIAA Atmospheric Flight Mechanics Conference, AIAA Paper 2006-6647, 2006.

[23] Culler, A., Williams, T., and Bolender, M., "Aerothermal Modeling and Dynamic Analysis of a Hypersonic Vehicle," AIAA Atmospheric Flight Mechanics Conference, AIAA Paper 2007-6395, 2007.

[24] Oppenheimer, M., Skijins, T., Bolender, M., and Doman, D., "A Flexible Hypersonic Vehicle Model Developed With Piston Theory," AIAA Atmospheric Flight Mechanics Conference, AIAA Paper 2007-6396, 2007.

[25] Jankovsky, P., Sigthorsson, D., Serrani, A., Yurkovich, S., Bolender, M., and Doman, D., "Output Feedback Control and Sensor Placement

for a Hypersonic Vehicle Model," AIAA Guidance, Navigation, and Control Conference, AIAA Paper 2007- 6327, 2007.

[26] Fiorentini, L., Serrani, A., Bolender, M., and Doman, D., "Nonlinear Robust/Adaptive Controller Design for an Air- Breathing Hypersonic Vehicle Model," AIAA Guidance, Navigation, and Control Conference, AIAA Paper 2007-6329, 2007.

[27] Lind, R., "Linear Parameter-Varying Modeling and Control of Structural Dynamics with Aeroelastic Effects," *Journal of Guidance, Control, and Dynamics*, Vol. 25, No. 4, 2002, pp. 733–739. doi:10.2514/2.4940

[28] Heeg, J., Zeiler, T. A., Pototzky, A. S., Spain, C. V., and Engelund, W. C., " Aerothermoelastic Analysis of a NASP Demonstrator Model," AIAA Paper 1993-1366.

[29] Heeg, J., Gilbert, M. G., and Pototzky, A. S., "Aerothermoelastic Effects for a Conceptual Hypersonic Aircraft," *Journal of Aircraft*, Vol. 30, No. 4, 1993, pp. 453–458. doi:10.2514/3.56890

A. Sinha
Associate Editor